JB
Journals.ASM.org

The Terminal Oxidase cbb_3 Functions in Redox Control of Magnetite Biomineralization in *Magnetospirillum gryphiswaldense*

Yingjie Li,[a] Oliver Raschdorf,[a,b] Karen T. Silva,[a] Dirk Schüler[c]

Ludwig Maximilians Universität München, Department Biologie I, Mikrobiologie, Planegg-Martinsried, Germany[a]; Max Planck Institute of Biochemistry, Department of Molecular Structural Biology, Martinsried, Germany[b]; Universität Bayreuth, Lehrstuhl f. Mikrobiologie, Bayreuth, Germany[c]

The biomineralization of magnetosomes in *Magnetospirillum gryphiswaldense* and other magnetotactic bacteria occurs only under suboxic conditions. However, the mechanism of oxygen regulation and redox control of biosynthesis of the mixed-valence iron oxide magnetite [FeII(FeIII)$_2$O$_4$] is still unclear. Here, we set out to investigate the role of aerobic respiration in both energy metabolism and magnetite biomineralization of *M. gryphiswaldense*. Although three operons encoding putative terminal cbb_3-type, aa_3-type, and *bd*-type oxidases were identified in the genome assembly of *M. gryphiswaldense*, genetic and biochemical analyses revealed that only cbb_3 and *bd* are required for oxygen respiration, whereas aa_3 had no physiological significance under the tested conditions. While the loss of *bd* had no effects on growth and magnetosome synthesis, inactivation of cbb_3 caused pleiotropic effects under microaerobic conditions in the presence of nitrate. In addition to their incapability of simultaneous nitrate and oxygen reduction, cbb_3-deficient cells had complex magnetosome phenotypes and aberrant morphologies, probably by disturbing the redox balance required for proper growth and magnetite biomineralization. Altogether, besides being the primary terminal oxidase for aerobic respiration, cbb_3 oxidase may serve as an oxygen sensor and have a further role in poising proper redox conditions required for magnetite biomineralization.

Magnetotactic bacteria (MTB) are capable of orientation in the Earth's magnetic field to search for their preferred low-oxygen environments, which is achieved by unique intracellular organelles, the magnetosomes (1). In the alphaproteobacterium *Magnetospirillum gryphiswaldense* (here referred to as MSR-1) and related MTB, magnetosomes comprise membrane-enveloped magnetite crystals and are aligned in chains (1). Previous studies revealed that magnetosome biosynthesis is largely controlled by a set of about 30 specific genes localized within the genomic magnetosome island (MAI) (2–5), whereas determinants encoded elsewhere play accessory roles in magnetite biomineralization (6, 7). The synthesis of the mixed-valence iron oxide magnetite [FeII(FeIII)$_2$O$_4$] was previously proposed to proceed by coprecipitation of balanced amounts of ferrous and ferric iron, which thus requires a precise biological regulation of intracellular redox conditions (8–10). In inorganic synthesis of magnetite films called ferrite plating, nitrite and oxygen have been shown to be potent oxidants for ferrous iron (11). One of the major redox pathways in microaerophilic MSR-1 was found to be denitrification, which is a respiratory process to stepwise reduce nitrate to N_2 (12). Our previous work showed that in MSR-1, denitrification plays an important role in poising redox conditions for magnetite biomineralization (6, 7). Deletion of *nap* genes encoding a periplasmic nitrate reductase not only abolished anaerobic growth and delayed aerobic growth but also severely affected magnetite synthesis and led to the formation of fewer, smaller, and irregular magnetosomes during denitrification and microaerobic oxygen respiration (6). Genetic inactivation of the nitrite reductase NirS resulted in defective growth and biosynthesis of smaller and irregular particles during nitrate reduction (7). In addition to denitrification, which occurs only under suboxic conditions, MSR-1 and related MTB are also capable of aerobic respiration using O_2 as the terminal electron acceptor. Although isotope experiments demonstrated that oxygen molecules bound in biologically synthesized Fe_3O_4 are derived from water but not O_2, it has been observed that the O_2 concentration is a crucial factor that significantly affects magnetosome biosynthesis (13). Magnetite crystals are biomineralized only under suboxic conditions, whereas atmospheric oxygen concentrations entirely inhibit the formation of magnetosomes (6, 14). However, the mechanism of oxygen regulation and redox control of magnetite biomineralization has remained unclear. By visible absorption spectroscopy, enzymes for respiration were identified in *Magnetospirillum magnetotacticum*, including *a*-, a_1-, *b*-, *c*-, cd_1-, and *o*-type cytochromes (15). More than 85% of the total cytochromes were of the *c* type, which were mainly soluble, whereas the *a*- and *b*-type cytochromes were detected mostly in cell membranes. Since a_1 hemes (usually part of the "low-aeration" cytochrome oxidase) and *o* hemes (usually part of the "high-aeration" cytochrome oxidase) were simultaneously observed in *M. magnetotacticum*, O'Brien et al. suggested that the oxygen respiration chain is branched (15). Subsequently, a new "cytochrome a_1-like" hemoprotein was found to display weak cytochrome *c* oxidase activity *in vitro* and to be present in larger amounts in magnetic than in nonmagnetic cells of *M. magnetotacticum*, suggesting that this protein might be involved in magnetosome formation (16). For the same organism, Tamegai and Fukumori in 1994 reported a novel *cbb*-type cytochrome *c* oxidase, which displayed cytochrome *c* oxidase activity and thus was assumed to function as the terminal oxidase for microaerobic respiration (17). However, until now, no genetic evidence has been available

Received 10 March 2014 **Accepted** 25 April 2014
Published ahead of print 2 May 2014
Address correspondence to Dirk Schüler, dirk.schueler@lrz.uni-muenchen.de.
Supplemental material for this article may be found at http://dx.doi.org/10.1128/JB.01652-14.
Copyright © 2014, American Society for Microbiology. All Rights Reserved.
doi:10.1128/JB.01652-14

to elucidate which proteins mediate oxygen respiration and whether aerobic respiration is involved in magnetite biomineralization.

In prokaryotes, there are two major groups of terminal oxidases involved in O_2 reduction: the universal cytochrome *c* oxidases and the quinol oxidases (18). All of cytochrome *c* oxidases, which relay electrons from cytochrome *c* to O_2, are members of heme-copper oxidases (HCOs). Based on evolutionary relationships, HCOs are classified into three different types: (i) type A oxidases, grouped as cytochrome oxidases aa_3, which are homologous to the mitochondrial oxidases (19); (ii) type B oxidases, in which the catalytic subunit and two other subunits are analogous to the subunits of aa_3-type cytochrome *c* oxidases (20); and (iii) type C oxidases, the cytochrome oxidases cbb_3. Unlike the oxidase aa_3, which functions under aerobic conditions, the cbb_3 oxidase encoded by the *ccoNOQP* operon is expressed primarily under O_2-limiting conditions, reflecting its high affinity for O_2 (21). The *bd*-type quinol oxidases provide an alternative branch and accept electrons directly from the quinol pool for O_2 reduction (18). Although *bd* quinol oxidases do not pump protons and therefore are less efficient at creating the charge gradient for ATP synthesis than HCOs, they have been found to have a higher affinity for O_2 than other cytochrome oxidases (22) and therefore were proposed to function under low-O_2 conditions (23). However, their physiological function has remained unclear.

Here, we set out to explore the role of O_2 and aerobic respiration in metabolism and magnetite biomineralization by mutagenesis of different terminal oxidases in MSR-1. Although three putative terminal oxidases were identified in MSR-1, only oxidases cbb_3 and *bd* were required for O_2 reduction, whereas cytochrome *c* oxidase aa_3 did not show any physiological function under our laboratory conditions. Genetic and biochemical analyses revealed that active aerobic respiration is essential for microaerobic denitrification, and the cbb_3 oxidase is required for simultaneous denitrification and aerobic respiration under microaerobic conditions. Moreover, besides being a primary terminal oxidase, cbb_3 is also involved in magnetite biomineralization, and its loss caused pleiotropic effects under microaerobic conditions in the presence of nitrate, such as significant delays of growth, severely impaired magnetite synthesis, and aberrant cell morphologies, probably by disturbing the intracellular redox state required for metabolism and magnetite biomineralization.

MATERIALS AND METHODS

Bacterial strains and growth conditions. Bacterial strains and plasmids used in these studies are listed in Table S1 in the supplemental material. *Escherichia coli* strains were routinely cultured in lysogeny broth (LB) at 37°C, and MSR-1 strains were grown at 30°C in nitrate medium if not specified otherwise (6). In ammonium medium, nitrate was replaced by 4 mM ammonium chloride. When needed, kanamycin was used at the following concentrations: 25 μg/ml for *E. coli* and 5 μg/ml for MSR-1. A total of 300 μM diaminopimelic acid (DAP) was added to the medium when *E. coli* strain BW29427 was used as the donor for conjugation.

Under anaerobic and microaerobic conditions, the optical density and magnetic response (C_{mag}) were measured spectrophotometrically at 565 nm in 300-ml bottles containing 50 ml medium, as previously described (24). For microaerobic conditions, before autoclaving, bottles were sealed with butyl-rubber stoppers and flushed with a microoxic gas mixture containing 2% O_2 and 98% N_2. Anaerobic conditions were achieved by omitting oxygen from the gas mixture. For aerobic conditions, cells were grown with free gas exchange with air in 500-ml flasks containing 40 ml medium agitated at 200 rpm. If not specified, inocula were prepared anaerobically.

Genetic and molecular biology techniques. Standard molecular and genetic techniques were used for DNA isolation, digestion, ligation, and transformation (25). All DNA products were sequenced by using BigDye Terminator version 3.1 chemistry on an ABI 3700 capillary sequencer (Applied Biosystems, Darmstadt, Germany). Sequence data were analyzed with Vector NTI Advance 11.5.1 software (Invitrogen, Darmstadt, Germany). All oligonucleotide sequences used in this work are available upon request.

Construction of mutant strains. First, the fused flanking sections of operons encoding cbb_3, aa_3, and *bd* oxidases were cloned into PstI/SpeI-digested pOR093 to yield pLYJ128, pLYJ129, and pLYJ130, respectively. Unmarked deletions of cbb_3, aa_3, and *bd* oxidase operons were performed by a two-step homologous recombination technique in the same manner as that described previously (41). After PCR screening, mutants were generated and finally designated the Δcbb_3, Δaa_3, and Δ*bd* mutants, respectively. For double deletion mutants, pLYJ128 was transformed into the Δaa_3 and Δ*bd* mutants by conjugation, and two different double mutants, the Δaa_3 Δcbb_3 and Δ*bd* Δcbb_3 mutants, respectively, were obtained. Plasmid pLYJ129 was transformed into the Δ*bd* mutant by conjugation to generate the Δ*bd* Δaa_3 double deletion mutant.

For genetic complementation of the Δcbb_3, Δaa_3 Δcbb_3, and Δ*bd* Δcbb_3 mutants, the *ccoNOQP* operon encoding cbb_3 oxidase with its own promoter region was ligated into HindIII/SmaI-digested pBBR1MCS-2 to obtain plasmid pLYJ138. In addition, as controls, operons encoding the respective aa_3 and *bd* oxidases were also complemented in the Δaa_3 Δcbb_3 mutant and Δ*bd* Δcbb_3 mutant. The PCR product of the *coxBAC* operon encoding aa_3 oxidase with its own promoter region was digested with HindIII and SmaI and further ligated into pBBR1MCS-2 to generate pLYJ139. The PCR fragment of the *cydAB* operon encoding *bd* oxidase with its own promoter region was digested with ApaI and SacI and also ligated into pBBR1MCS-2 to generate plasmid pLYJ140.

Analysis of transcriptional *gusA* fusions. To investigate the transcription of different terminal oxidases under different conditions, promoter regions of the *ccoNOQP*, *coxBAC*, and *cydAB* operons were cloned into Acc65I/HindIII-digested pLYJ97, and the resulting plasmids were designated pLYJ115, pLYJ135, and pLYJ137, respectively. Also, β-glucuronidase activity was determined at 37°C as described previously (6). Triplicate assays were performed, and the values reported were averaged by using at least two independent experiments.

Nadi assay. The *N,N*-dimethyl-*p*-phenylenediamine (Nadi) assay was used for the detection of cytochrome *c* oxidase activity (26). A mixture of 1% α-naphthol (Sigma-Aldrich) in ethanol and 1% *N,N*-dimethyl-*p*-phenylenediamine monohydrochloride (Sigma-Aldrich) was applied to cover colonies. Strains containing an active cytochrome *c* oxidase turn blue within 5 min.

Nitrate and nitrite concentration assays. Different strains were grown under microaerobic conditions in the presence of nitrate. One milliliter of culture at different time points was used to detect nitrate and nitrite concentrations, as described previously (6). Duplicate assays were carried out, and the values reported were measured in one representative experiment.

NAD^+/NADH ratio assay. Different strains were grown in nitrate or ammonium medium under different conditions and harvested at an optical density at 565 nm (OD_{565}) of 0.1 to 0.2. Each culture, containing about 10^5 cells, was suspended in 50 μl phosphate-buffered saline (PBS) buffer and subjected to extraction and detection by using an NAD/NADH-Glo assay (Promega) according to the manufacturer's instructions. Luminescence was recorded by using a Synergy 2 multimode microplate reader from BioTek.

Transmission electron microscopy (TEM). MSR-1 wild-type (WT) and mutant strains were grown at 30°C under different conditions, concentrated, and adsorbed onto carbon-coated copper grids. Samples were viewed and recorded with an FEI CM200 microscope (FEI, Eindhoven,

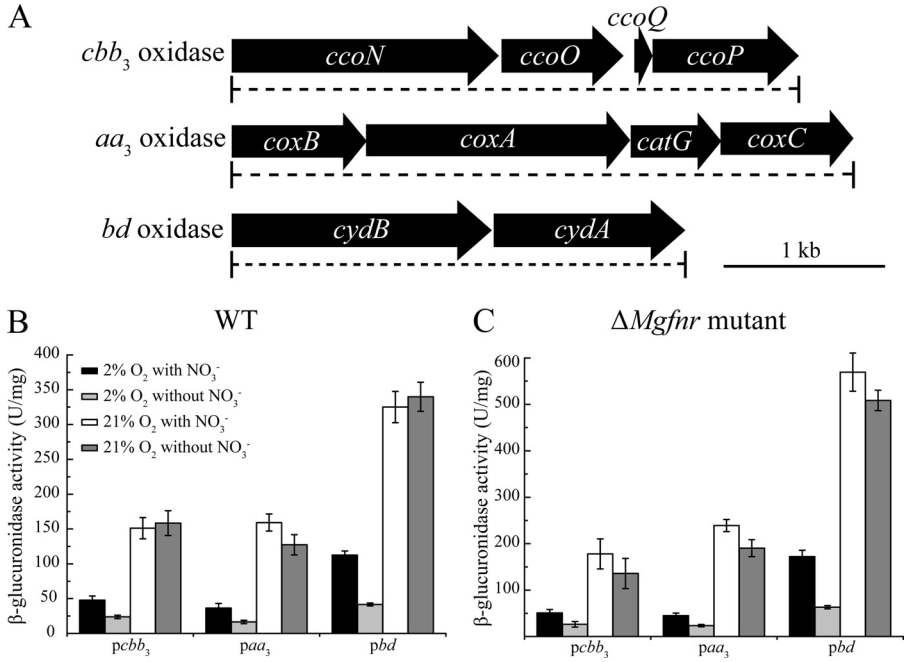

FIG 1 (A) Molecular organization of putative terminal oxidase in the genome assembly of MSR-1. Dashed lines indicate the extent of deletions in mutant strains. (B and C) Transcription of putative terminal oxidase operons with *gusA* as a reporter in WT (B) and Δ*Mgfnr* mutant (C) cells. Cultures were grown aerobically (21% O_2) in nitrate and ammonium medium or microaerobically (2% O_2) in nitrate and ammonium medium. Expression was measured by β-glucuronidase activities.

Netherlands), using an accelerating voltage of 160 kV, or a Morgagni 268 microscope (FEI, Eindhoven, Netherlands) at 80 kV.

Sequence analysis. Genes encoding different oxygen terminal oxidase genes were identified by BLASTP (http://blast.ncbi.nlm.nih.gov/Blast.cgi) homology searching in the genomes of MSR-1 (GenBank accession number CU459003.1), *Magnetospirillum magneticum* (GenBank accession number AP007255.1), *M. magnetotacticum* (NCBI reference sequence NZ_AAAP00000000.1), *Magnetococcus marinus* (GenBank accession number CP000471.1), and *Desulfovibrio magneticus* strain RS-1 (GenBank accession number AP010904.1).

RESULTS

Identification of terminal oxidases involved in aerobic respiration. Three operons encoding putative terminal cbb_3-type, aa_3-type, and *bd*-type oxidases were identified in the draft genome assembly of MSR-1 (Fig. 1A). cbb_3 and aa_3 oxidases, encoded by their respective operons *ccoNOQP* and *coxBAC*, belong to the family of cytochrome *c* oxidases. In some bacteria, aa_3 is the predominant oxidase under O_2-rich growth conditions, whereas cbb_3 is expressed only under conditions of O_2 limitation (27). Although *ccoNOQP* operons are also present in other MTB, including *M. magneticum*, *M. magnetotacticum*, and *Mc. marinus*, some genes are absent from their *ccoNOQP* operons (see Table S2 in the supplemental material). A *coxBAC* operon is present in *M. magneticum* and *M. magnetotacticum*, whereas none of the *coxBAC* genes were detected in *Mc. marinus*, which is capable of only microaerobic and not aerobic or anaerobic growth, suggesting that aa_3 oxidase might not be necessary for microaerobic O_2 reduction. Cytochrome *c* oxidases appear to be absent from the magnetotactic bacterium *D. magneticus* (see Table S2 in the supplemental material), which utilizes sulfate and fumarate but not nitrate or O_2 as terminal electron acceptors (28). The third oxidase identified in MSR-1, *bd* oxidase, encoded by a *cydAB* operon, is a member of the quinol oxidase family, which is able to accept electrons for O_2 reduction directly from the quinol pool. However, we failed to detect any *cydAB* homologs in the genomes of other MTB except for *D. magneticus* (see Table S2 in the supplemental material). Despite the distinct content and organization of genes encoding oxygen-reducing enzymes, all known magnetospirilla are capable of growth under both microaerobic and aerobic conditions with O_2 as the electron acceptor (14), indicating that different branches for aerobic respiration might occur in different magnetospirilla.

MgFnr-independent expression of *ccoNOQP*, *coxBAC*, and *cydAB* operons is upregulated by oxygen. Since the three putative terminal oxidases in other bacteria were reported previously to show distinct affinities for oxygen and thus exhibit their maximum expression levels at different oxygen concentrations (27), we tested their expression patterns in WT MSR-1 under different conditions (Fig. 1B). By transcriptional *gusA* fusions, we found that the expression of all putative terminal oxidase operons was upregulated by oxygen, and the highest levels of β-glucuronidase activity were detected under aerobic conditions, whereas nitrate did not affect their aerobic expression. Under microaerobic conditions, an ~2-fold-higher level of β-glucuronidase activity was observed in the presence of nitrate than in its absence (Fig. 1B). In other bacteria, Fnr as a global regulator is known to play a key role in controlling the transcription of aerobic respiration genes (27, 29), which raised the question of whether Fnr in MSR-1 (named MgFnr) is involved in regulating the expression of these terminal oxidase operons in response to variable O_2 concentrations. Therefore, we performed the same experiments in a Δ*Mgfnr* mutant, in which deregulated expression of several denitrification genes (*nirS*, *nor*, and *nosZ*) under aerobic conditions was recently observed (Y. Li, M. Sabaty, S. Borg, K. T. Silva, D. Pignol, and D. Schüler, submitted for publication). As shown in Fig. 1C, Δ*Mgfnr*

TABLE 1 Phenotypic characterization of different terminal oxidase mutants[a]

Strain	Phenotype under conditions of:				
	0% O_2	2% O_2, +NO_3^-	2% O_2, +NH_4^+	21% O_2, +NO_3^-	21% O_2, +NH_4^+
Δaa_3	WT-like	WT-like	WT-like	WT-like	WT-like
Δ*bd*	WT-like	WT-like	WT-like	WT-like	WT-like
Δ*bd* Δaa_3	WT-like	WT-like	WT-like	WT-like	WT-like
Δcbb_3	WT-like	Delayed growth Severely impaired biomineralization Aberrant shape of cells	Delayed growth Weakly impaired biomineralization	Delayed growth	Delayed growth
Δaa_3 Δcbb_3	WT-like	Delayed growth Severely impaired biomineralization Aberrant shape of cells	Delayed growth Weakly impaired biomineralization	Delayed growth	Delayed growth
Δ*bd* Δcbb_3	WT-like	No growth	No growth	No growth	No growth

[a] WT-like indicates that growth and magnetite biomineralization are not visibly different from those of the WT; delayed growth indicates that cells grew slowly compared to the WT. Phenotypes of mutants different from that of the WT are indicated by shading.

cells carrying *ccoNOQP-gusA* (pLYJ115), *coxBAC-gusA* (pLYJ135), and *cydAB-gusA* (pLYJ137) showed the same expression patterns as the WT. For example, oxygen increased β-glucuronidase activity, while nitrate did not affect aerobic expression, and microaerobically grown Δ*Mgfnr* cells exhibited higher levels of β-glucuronidase activity in the presence of nitrate than in its absence. Altogether, these data suggested that in MSR-1, the transcription of putative terminal oxidases is not under the control of MgFnr, and thus, other unknown regulators likely mediate their expression in response to different O_2 concentrations.

Loss of both *cbb*$_3$ and *bd* but not *aa*$_3$ abolishes growth in the presence of oxygen, and aerobic respiration is a prerequisite for microaerobic denitrification. To determine whether the *cbb*$_3$, *aa*$_3$, and *bd* oxidases fulfill similar physiological functions and whether they are involved in magnetite biomineralization, we constructed several mutants, including Δ*cbb*$_3$, Δ*aa*$_3$, and Δ*bd* single-operon deletions and Δ*bd* Δ*aa*$_3$, Δ*aa*$_3$ Δ*cbb*$_3$, and Δ*bd* Δ*cbb*$_3$ double deletions. Upon repeated attempts, Δ*cbb*$_3$, Δ*aa*$_3$ Δ*cbb*$_3$, and Δ*bd* Δ*cbb*$_3$ mutants could be obtained only when the entire selection procedure (e.g., plating and cultivation of colonies) was performed under strictly anaerobic conditions. Phenotypes of all mutants with respect to growth and magnetite biomineralization are summarized in Table 1 and Table S3 in the supplemental material. Hardly any difference in growth was observed between the Δ*aa*$_3$, Δ*bd*, and Δ*bd* Δ*aa*$_3$ mutants and the WT under all tested conditions. Under aerobic conditions, WT cells grew to stationary phase within about 24 h in both nitrate and ammonium media, whereas the Δ*cbb*$_3$ and Δ*aa*$_3$ Δ*cbb*$_3$ mutants required about 120 to 140 h to grow to WT-like cell densities (Fig. 2A and B). When the Δ*cbb*$_3$ and Δ*aa*$_3$ Δ*cbb*$_3$ strains were incubated microaerobically in ammonium medium, stationary phase was reached by both mutants 3 h later than the WT (Fig. 2C). In microaerobic nitrate medium, the Δ*cbb*$_3$ and Δ*aa*$_3$ Δ*cbb*$_3$ mutants showed even larger lags of about 12 h to reach the stationary phase (Fig. 3A). Taken together, based on the observations that the Δ*cbb*$_3$ and Δ*aa*$_3$ Δ*cbb*$_3$ mutants had similar phenotypes (delayed growth) while the Δ*aa*$_3$ mutant did not show any growth impairment, we concluded that the *aa*$_3$ oxidase in MSR-1 has no physiological significance for aerobic respiration. In agreement with this, in the Δ*bd* Δ*cbb*$_3$ double deletion mutant, no growth was observed under microaerobic or aerobic conditions (Table 1), demonstrating that *cbb*$_3$ and *bd* but not *aa*$_3$ function in O_2 reduction. The observation that the Δ*bd* Δ*cbb*$_3$ mutant did not grow microaerobically even in the presence of nitrate also indicated that aerobic respiration is a prerequisite to activate the microaerobic denitrification pathway. Furthermore, loss of *bd* oxidase did not affect microaerobic or aerobic growth, whereas loss of *cbb*$_3$ oxidase caused severely impaired microaerobic and aerobic growth, suggesting that compared to *bd* oxidase, the *cbb*$_3$ oxidase plays a pronounced role in aerobic respiration under both O_2-rich and O_2-limited conditions.

To further prove that *cbb*$_3$ but not *aa*$_3$ is the only physiologically functional cytochrome *c* oxidase, we performed the Nadi assay, which is commonly used to specifically detect cytochrome *c* oxidase activity (26). Using *N*,*N*-dimethyl-*p*-phenylenediamine monohydrochloride as an exogenous electron donor, cytochrome *c* oxidase is able to catalyze the rapid formation of indophenol blue from colorless α-naphthol. As shown in Fig. 4A, the Δ*aa*$_3$, Δ*bd*, and Δ*bd* Δ*aa*$_3$ strains showed reaction rates similar to those of the WT, forming indophenol blue visibly within <1 min and developing maximum coloration within 5 min. However, all *cbb*$_3$-deficient mutants, including the Δ*cbb*$_3$, Δ*aa*$_3$ Δ*cbb*$_3$, and Δ*bd* Δ*cbb*$_3$ mutants, did not exhibit any indophenol blue formation. Only when colonies were complemented with plasmid pLYJ138, containing a WT *cbb*$_3$ allele, did they form indophenol blue, indicating that *cbb*$_3$ itself is sufficient to rescue the cytochrome *c* oxidase activity (Fig. 4B). However, the formation of indophenol blue was not restored in the Δ*aa*$_3$ Δ*cbb*$_3$ and Δ*bd* Δ*cbb*$_3$ mutants by complementation with the respective WT (*aa*$_3$, pLYJ139; *bd*, pLYJ140) allele (Fig. 4B). These data demonstrated again that only cytochrome *c* oxidase *cbb*$_3$, but not *aa*$_3$, is capable of O_2 reduction.

Loss of *cbb*$_3$ impairs magnetite biomineralization and causes aberrant cell morphologies under microaerobic conditions in the presence of nitrate. Compared to the WT, the Δ*aa*$_3$, Δ*bd*, and Δ*bd* Δ*aa*$_3$ mutants showed a similar magnetic response (C_{mag}) and size, number, and appearance of magnetosomes under anaerobic and microaerobic conditions (see Table S3 in the supplemental material). Likewise, the Δ*cbb*$_3$, Δ*aa*$_3$ Δ*cbb*$_3$, and Δ*bd* Δ*cbb*$_3$ mutants also displayed WT-like C_{mag} values and magnetosome sizes and morphologies under anaerobic conditions (see Table S3 in the supplemental material). Under microaerobic conditions in the absence of nitrate, the average C_{mag} values of the Δ*cbb*$_3$ and Δ*aa*$_3$ Δ*cbb*$_3$ mutants were slightly lower than that of the WT during the entire growth period (Fig. 2C). TEM revealed that both Δ*cbb*$_3$ and Δ*aa*$_3$ Δ*cbb*$_3$ cells synthesized slightly smaller magnetosomes only at the beginning of growth (6 h), whereas in the following period, the average particle size in both mutants was not different from

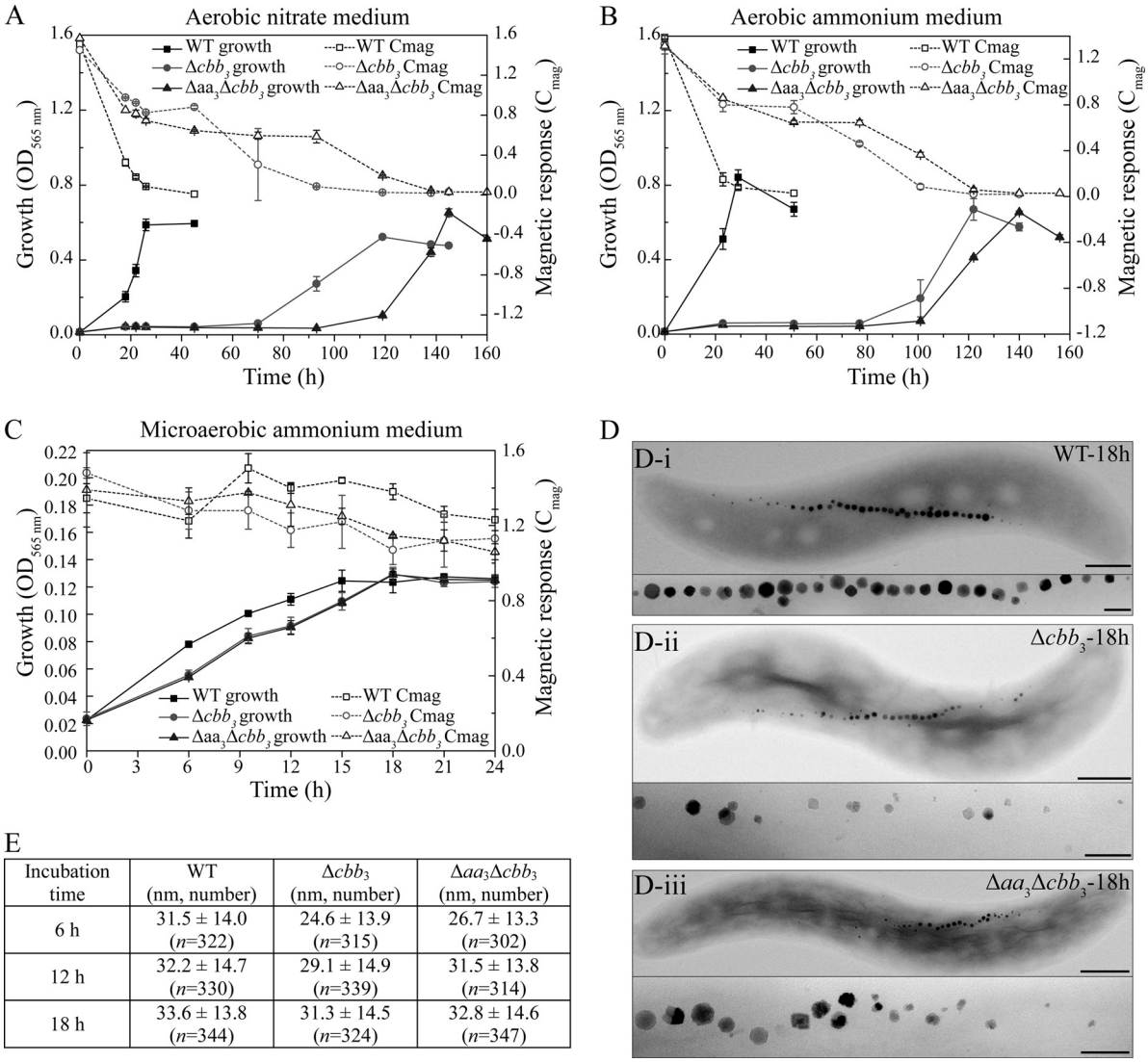

E

Incubation time	WT (nm, number)	Δ*cbb*$_3$ (nm, number)	Δ*aa*$_3$Δ*cbb*$_3$ (nm, number)
6 h	31.5 ± 14.0 (*n*=322)	24.6 ± 13.9 (*n*=315)	26.7 ± 13.3 (*n*=302)
12 h	32.2 ± 14.7 (*n*=330)	29.1 ± 14.9 (*n*=339)	31.5 ± 13.8 (*n*=314)
18 h	33.6 ± 13.8 (*n*=344)	31.3 ± 14.5 (*n*=324)	32.8 ± 14.6 (*n*=347)

FIG 2 (A to C) Growth (OD_{565}) and magnetic response (C_{mag}) of MSR-1 WT, Δ*cbb*$_3$, and Δ*aa*$_3$ Δ*cbb*$_3$ strains under different conditions. (A) Aerobic conditions in nitrate medium; (B) aerobic conditions in ammonium medium; (C) microaerobic conditions in ammonium medium. (D) TEM images of microaerobically grown WT (i), Δ*cbb*$_3$ mutant (ii), and Δ*aa*$_3$ Δ*cbb*$_3$ mutant (iii) strains in ammonium medium. Bars, 500 nm (whole cells) and 100 nm (magnetosomes). (E) Measurements of crystal sizes for MSR-1 WT, Δ*cbb*$_3$, and Δ*aa*$_3$ Δ*cbb*$_3$ strains at different time points in microaerobic ammonium medium. Results from representative experiments were determined in triplicate, and values are given as means and standard deviations.

that in the WT (Fig. 2E). However, the magnetosome morphology in these two mutants was variable, including regular particles in the middle of chains in addition to small and irregular crystals at the ends of chains (Fig. 2D), which likely caused reduced C_{mag} values. In microaerobic nitrate medium, the loss of *cbb*$_3$ oxidase resulted in significantly lower C_{mag} values, which gradually decreased further during the entire growth period (Fig. 3A). In agreement with this, magnetosomes in the Δ*cbb*$_3$ and Δ*aa*$_3$ Δ*cbb*$_3$ mutants were much smaller than those in the WT, and this difference became more obvious as growth proceeded at later stages (Fig. 3C). In addition, the phenotypes were inconsistent and displayed various distinct types of magnetosome formation and organization (Fig. 5; see also Fig. S1 in the supplemental material): (i) type 1, consisting of magnetosome chains containing WT-like particles in the middle flanked by small, irregular particles at each end (≥3 WT-like particles in the middle) (Fig. 5Ai to Di); (ii) type 2, consisting of magnetosomes appearing as much smaller and irregularly shaped particles, which were arranged in loose chains (≤2 WT-like particles) (Fig. 5Aii to Dii); and (iii) type 3, consisting of two loose magnetosome chains present at each side of the cell (Fig. 5Aiii to Diii). These two chains furthermore exhibited two different appearances: one contained two type 2 chains, which had only smaller and irregular particles (Fig. 5Aiii and Biii), and the other consisted of one type 1 chain and one type 2 chain (Fig. 5Ciii and Diii). Similar phenotypes were observed at different growth points, including Δ*cbb*$_3$ and Δ*aa*$_3$ Δ*cbb*$_3$ cells cultured for 9 h (Fig. 5), 18 h, 24 h, 29 h, and 35 h (TEM images of cells grown for 24 h and 35 h are shown in Fig. S1 in the supplemental material). However, the proportion of type 1 magnetosomes was reduced at later growth stages (Fig. 3D), which probably resulted in a decreased average size of particles during growth.

In addition, light microscopy (data not shown) and TEM also

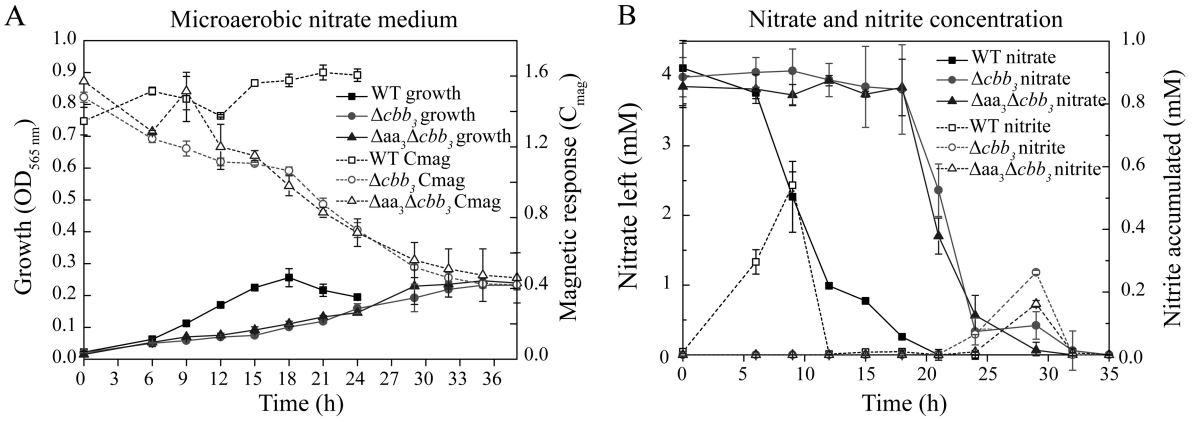

C

Incubation time	WT (nm, number)	Δcbb_3 (nm, number)	$\Delta aa_3\Delta cbb_3$ (nm, number)
9 h	29.3 ± 18.6 (*n*=347)	15.2 ± 13.1 (*n*=355)	14.7 ± 14.2 (*n*=308)
18 h	27.6 ± 18.7 (*n*=352)	12.8 ± 13.8 (*n*=312)	11.1 ± 11.8 (*n*=319)
24 h	33.6 ± 14.9 (*n*=372)	10.2 ± 10.9 (*n*=316)	11.7 ± 11.9 (*n*=317)
29 h	-	10.4 ± 9.3 (*n*=335)	9.5 ± 11.0 (*n*=313)
35 h	-	11.2 ± 9.6 (*n*=322)	8.2 ± 8.0 (*n*=363)

D

Incubation time	Δcbb_3				$\Delta aa_3\Delta cbb_3$			
	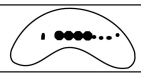	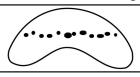	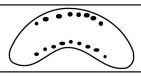	*n*			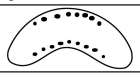	*n*
9 h	75%	18%	7%	60	79%	20%	2%	115
18 h	69%	15%	16%	67	66%	25%	10%	122
24 h	50%	34%	16%	74	60%	26%	14%	182
29 h	48%	38%	14%	134	37%	36%	28%	133
35 h	47%	35%	18%	100	39%	32%	29%	103

FIG 3 (A) Growth (OD_{565}) and magnetic response (C_{mag}) of MSR-1 WT, Δcbb_3, and Δaa_3 Δcbb_3 strains in microaerobic nitrate medium. (B) Time courses of nitrate and nitrite utilization during microaerobic growth in nitrate medium. (C) Measurements of crystal sizes for MSR-1 WT, Δcbb_3, and Δaa_3 Δcbb_3 strains at different time points in microaerobic nitrate medium. The number of crystals measured for each strain (*n*) is shown. (D) Magnetosome morphotypes in Δcbb_3 and Δaa_3 Δcbb_3 mutants and proportion of each morphotype at different time points. The number of cells measured for each strain is presented.

showed that the morphology of Δcbb_3 and Δaa_3 Δcbb_3 cells (n = 300) was variable under microaerobic conditions in the presence of nitrate: (i) only <10% of cells showed a WT-like spiral shape (Fig. 6Ai and ii); (ii) about 30% were thicker spirals (>0.7-μm versus 0.5- to 0.6-μm diameter in the WT) (Fig. 6Bi and ii), and (iii) >60% of cells were thicker vibrioid cells (Fig. 6Ci and ii and Di and ii).

Transcomplementation of the Δcbb_3 and Δaa_3 Δcbb_3 mutants with a WT cbb_3 allele (pLYJ138) restored magnetosome formation and cell morphology back to WT-like levels in microaerobic nitrate medium (Fig. 4C and D). Taken together, these data indicated that besides its function in aerobic respiration, cbb_3 oxidase also functions in magnetosome formation under microaerobic conditions. The loss of cbb_3 oxidase caused a pronounced impairment of magnetite biomineralization and disturbed cell morphology in the presence of nitrate, which suggested that cytochrome *c* oxidase cbb_3 is more important in controlling magnetosome formation when denitrification and oxygen respiration overlap.

Cytochrome *c* oxidase cbb_3 functions to maintain proper redox conditions for magnetosome formation. Since the loss of only cbb_3 oxidase led to delayed microaerobic and aerobic growth and impaired magnetite biomineralization, we set out to further clarify its function. The observation that both the Δcbb_3 and Δaa_3 Δcbb_3 mutants displayed a more substantial lag of microaerobic growth in the presence of nitrate than in its absence prompted us to first monitor the denitrification process in these two strains during growth in microaerobic sealed flasks (Fig. 3B). WT cells started to reduce nitrate after about 6 h and then consumed all nitrate within the following 12 to 14 h, after which growth ceased, probably due to the depletion of both nitrate and oxygen. This finding, combined with the observation that in microaerobic ammonium medium, WT cells also took about 15 h to reach stationary phase, suggested that denitrification and aerobic respiration occurred simultaneously under microaerobic conditions, similar to what was observed in our previous study (6). During the entire growth period for the WT, a maximum concentration of about 0.5 mM nitrite was built up during the first 12 h. Unexpectedly, Δcbb_3

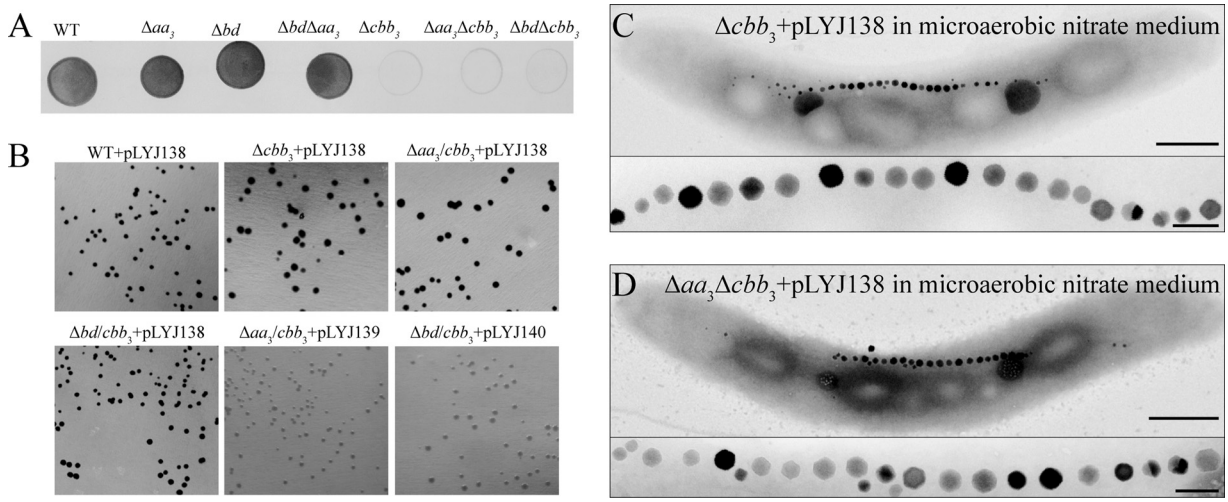

FIG 4 (A) Nadi assay of the WT and various mutant strains. This method is commonly used to specifically detect cytochrome *c* oxidase activity (26), which is based on the rapid formation of indophenol blue from colorless α-naphthol catalyzed by cytochrome *c* oxidases with *N*,*N*-dimethyl-*p*-phenylenediamine monohydrochloride as an exogenous electron donor. Five microliters of cultures grown anaerobically for 24 h, which were adjusted to about 10^7 CFU/ml, were dropped onto an agar plate in the presence of nitrate. Strains were incubated at 30°C for 4 days under anaerobic conditions and photographed after a 5-min Nadi reaction. (B) Nadi assay of anaerobically grown complementation strains. Plasmid pLYJ138 contains a WT cbb_3 allele, while pLYJ139 and pLYJ140 harbor WT aa_3 and *bd* alleles, respectively. (C) TEM images of Δcbb_3 and Δaa_3 Δcbb_3 strains complemented with plasmid pLY138, harboring the WT cbb_3 allele, grown in microaerobic nitrate medium. Bars, 500 nm (whole cells) and 100 nm (magnetosomes).

and Δaa_3 Δcbb_3 mutant cells were unable to reduce nitrate during the first 15 to 18 h, and only O_2-dependent growth occurred with a maximum OD of about 0.11, which was similar to the final OD of about 0.12 in microaerobic ammonium medium after 15 h of incubation. This implied that oxygen had to be nearly completely depleted after about 18 h before nitrate reduction became detectable. Nitrate then gradually disappeared within 15 to 18 h, and the Δcbb_3 and Δaa_3 Δcbb_3 mutants reached a final OD of about 0.25, which was similar to that of stationary WT cells. These findings revealed that cbb_3 oxidase is required for microaerobic conditions when denitrification and aerobic respiration occur simultaneously.

On the other hand, in the alphaproteobacterium *Rhodobacter sphaeroides*, it was shown previously that besides being a terminal oxidase, the cbb_3 oxidase also functions as an O_2 sensor to control the expression of photosynthesis genes (29–32). Therefore, we hypothesized that cbb_3 oxidase of MSR-1 may also sense O_2 to simultaneously activate and balance denitrification and aerobic respiration and, thus, to maintain proper redox conditions for magnetite synthesis under microaerobic conditions. To test our hypothesis, we determined the NAD^+ (oxidized)/NADH (reduced) ratio in the WT, Δcbb_3, and Δaa_3 Δcbb_3 strains because NAD as a coenzyme is an important redox factor involved in multiple redox reactions. Variable ratios of NAD^+/NADH corresponding to different oxygen concentrations were observed for the WT (Fig. 7). WT cells showed >2-fold-higher ratios of NAD^+/NADH under microaerobic than under anaerobic conditions, which indicated that anaerobiosis, as expected, caused a more reduced redox state. The absence of any difference between WT cultures grown with and those grown without nitrate under microaerobic conditions suggested that oxygen respiration plays a primary role in maintaining a proper ratio of NAD^+/NADH. Although oxygen reduction catalyzed by *bd* quinol oxidase still occurred in the Δcbb_3 mutant, the ratio of NAD^+/NADH under microaerobic conditions did not significantly increase compared to that under anaerobic conditions, indicating that *bd* oxidase is not involved in the regulation of redox conditions. The Δaa_3 Δcbb_3 mutant displayed a similar pattern, with hardly different ratios of NAD^+/NADH under anaerobic and microaerobic conditions. The ratios of NAD^+/NADH in both the Δcbb_3 and Δaa_3 Δcbb_3 strains under microaerobic conditions were much lower than those of the WT, implying a more reduced cellular redox state in the Δcbb_3 and Δaa_3 Δcbb_3 strains. Although the Δcbb_3 and Δaa_3 Δcbb_3 strains under microaerobic conditions did not reduce nitrate until oxygen was completely consumed, a similar ratio of NAD^+/NADH of about 3 to 4 was obtained at all tested stages of growth. Our data altogether suggest that cbb_3 oxidase is able to regulate redox conditions, thereby activating denitrification and controlling the biosynthesis of magnetite when O_2 is still available.

DISCUSSION

Consistent with our previously reported findings that deletion of *Mgfnr* affected neither oxygen consumption nor microaerobic magnetite biomineralization in the absence of nitrate (Li et al., submitted), we found that the expression level of the three cbb_3, aa_3, and *bd* terminal oxidase operons was increased by O_2 but not regulated by the global oxygen sensor MgFnr, similar to what was shown previously for *Shewanella oneidensis* (33). This suggested that some as-yet-unknown O_2 regulators probably mediate the expression of aerobic terminal oxidase genes in response to different oxygen concentrations. Mutagenesis of different terminal oxidases demonstrated that either of the cytochrome oxidases cbb_3 and *bd* is required for aerobic respiration, whereas aa_3 oxidase has no physiological significance for O_2 reduction under all tested conditions. This was further confirmed by the identical phenotypes of the Δcbb_3 and Δaa_3 Δcbb_3 strains. In their natural habitats of chemically stratified aquatic sediments, MTB such as MSR-1 are adapted to low-O_2 conditions (34), under which high-affinity

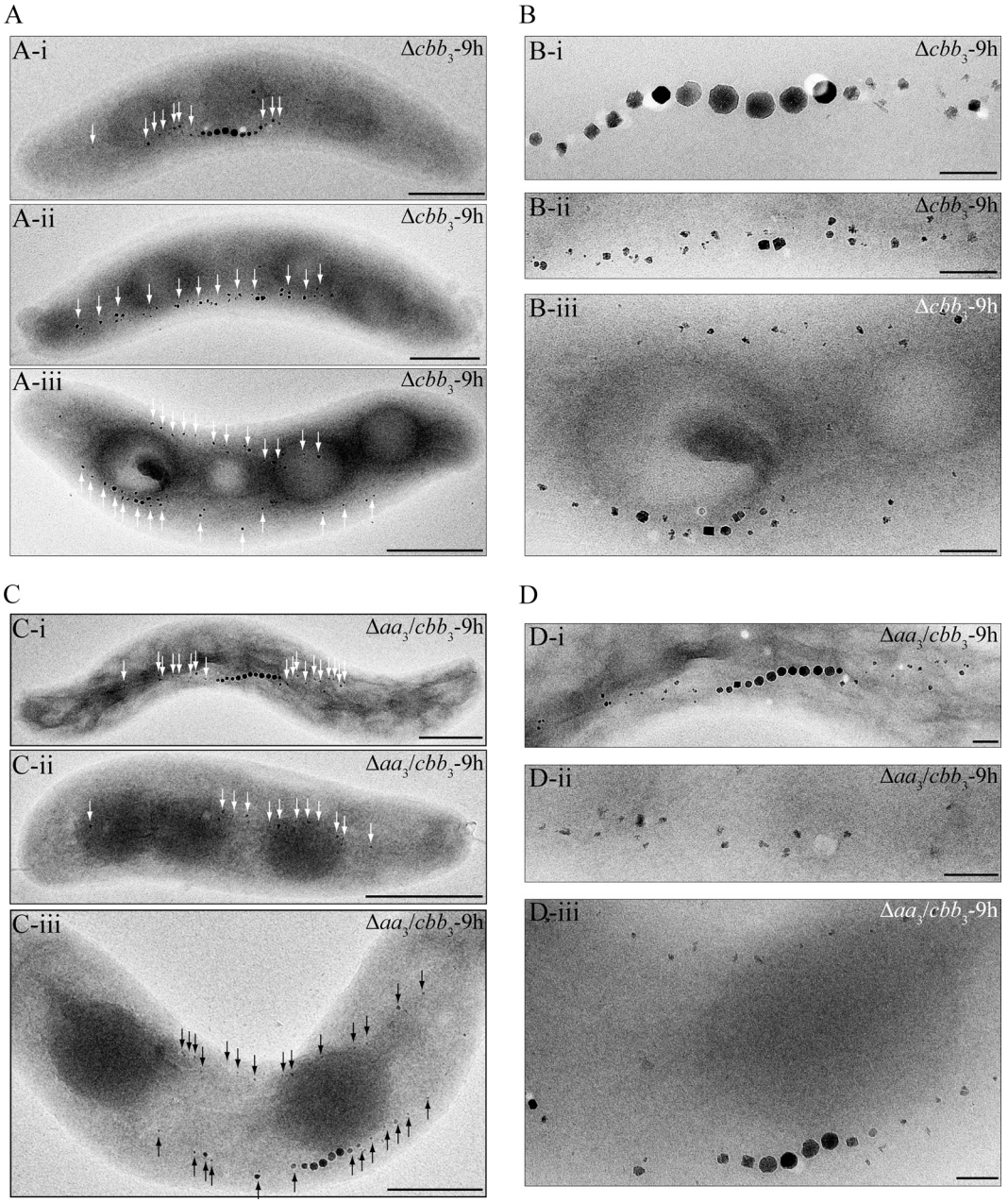

FIG 5 Biomineralization phenotypes of Δ*cbb*$_3$ and Δ*aa*$_3$ Δ*cbb*$_3$ mutants incubated for 9 h in microaerobic nitrate medium. (A and C) TEM images of whole cells of the Δ*cbb*$_3$ (A) and Δ*aa*$_3$ Δ*cbb*$_3$ (C) mutants. Bar, 500 nm. (B and D) Close-up views of magnetosome crystals shown in panels A and C, respectively. Bar, 100 nm. Irregularly shaped particles are indicated by arrows.

terminal oxidases like *cbb*$_3$ are favorable for O_2 respiration and energy conservation. In contrast, the *aa*$_3$ oxidase, which has a low affinity for O_2 (27), is insufficient to utilize trace amounts of O_2. Therefore, it is not surprising that *aa*$_3$ oxidase did not show any relevance for O_2 reduction. However, we cannot exclude the possibility that *aa*$_3$ oxidase has a function under certain environmental conditions, such as for O_2 detoxification in O_2-rich environments.

Based on the observation that a Δ*bd* Δ*cbb*$_3$ double deletion mutant did not grow in the presence of oxygen, we concluded that aerobic respiration is a prerequisite for microaerobic denitrification. The loss of the *bd* oxidase alone did not affect growth and magnetite biomineralization, which indicated that when *cbb*$_3$ oxidase is present, the *bd* oxidase might provide only a minor contribution to aerobic respiration. However, it is also possible that the activity of the *bd* oxidase is induced only when *cbb*$_3$ oxidase is eliminated to compensate for its loss. Unlike *cbb*$_3$ and *aa*$_3$ oxidases, which are present in the related magnetospirilla *M. magneticum* and *M. magnetotacticum*, *bd* oxidase is completely absent from these strains. This implies that *bd* oxidase is likely dispensable in various MTB, and *aa*$_3$ probably acts as an alternative terminal oxidase in these two magnetospirilla, while in *Mc. marinus*,

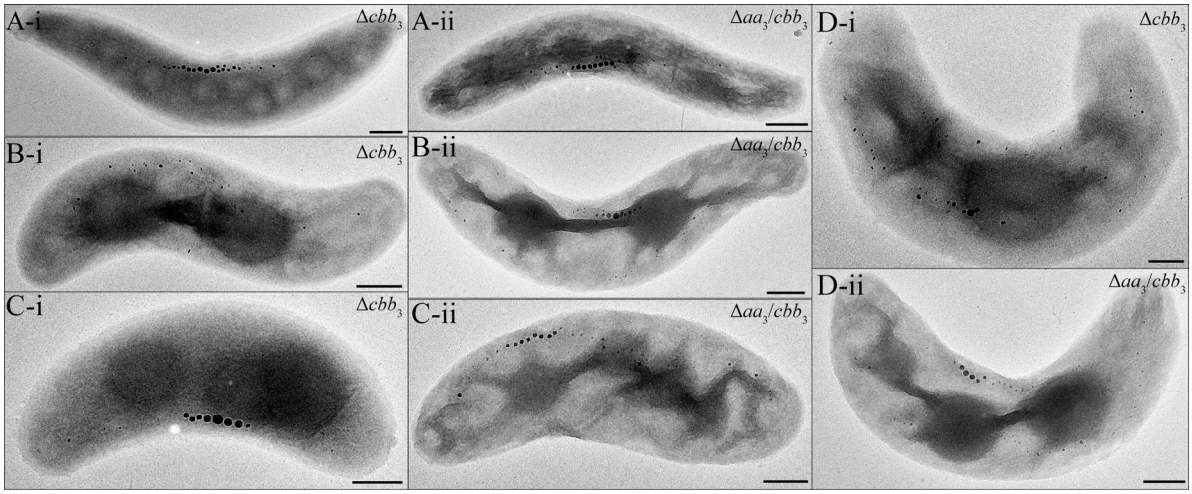

FIG 6 Morphologies found in different cells of the Δ*cbb*$_3$ and Δ*aa*$_3$ Δ*cbb*$_3$ mutants in microaerobic nitrate medium. (A) WT-like spiral-shaped mutant cells; (B) thicker spiral cells; (C and D) thicker and smaller vibrioid cells. Bar, 500 nm.

which is unable to grow aerobically, neither *bd* nor *aa*$_3$ oxidase is present. Nevertheless, *bd* oxidase might have unknown functions in MSR-1, whereas *cbb*$_3$ oxidase may be the only functional enzyme for aerobic respiration in *M. magneticum* and *M. magnetotacticum*.

The Δ*cbb*$_3$ and Δ*aa*$_3$ Δ*cbb*$_3$ mutants showed delayed growth in microaerobic ammonium medium. This might be caused by the low efficiency of *bd* oxidase, which is not able to pump protons but accepts only electrons directly from the quinol pool for O_2 reduction, while cytochrome *c* oxidase *cbb*$_3$ is more efficient at creating the charge gradient for ATP synthesis via the *bc-c-cbb*$_3$ branch (22). An even stronger delay of growth was observed for the Δ*cbb*$_3$ and Δ*aa*$_3$ Δ*cbb*$_3$ mutants in microaerobic nitrate medium. Unexpectedly, under these conditions, mutant cells did not start to reduce nitrate until O_2 was completely depleted, which suggested that the *cbb*$_3$ oxidase *per se*, but not aerobic respiration, is crucial for simultaneous O_2 and nitrate reduction. This finding therefore indicated that besides its role as a terminal oxidase, *cbb*$_3$ may be capable of sensing O_2 and may have a further key function in activating and maintaining simultaneous denitrification and aerobic respiration under microaerobic conditions. In microaerobic nitrate medium during early growth, only aerobic respiration prevailed (similar to conditions in microaerobic ammonium medium), while during later growth, only denitrification occurred, and mutant cells showed growth similar to that of anaerobically incubated WT cells. However, biomineralization phenotypes of the Δ*cbb*$_3$ and Δ*aa*$_3$ Δ*cbb*$_3$ mutants under these conditions were much different from those in either microaerobic ammonium medium or anaerobic nitrate medium. Thus, we can rule out that the severe defects in magnetite synthesis in the Δ*cbb*$_3$ and Δ*aa*$_3$ Δ*cbb*$_3$ mutants are caused by the incapability of a cooccurrence of denitrification and aerobic respiration. Instead, severely impaired magnetosome formation likely results from the loss of *cbb*$_3$ oxidase *per se*, which argues for a more direct role of this enzyme in magnetite biomineralization. In *R. sphaeroides*, besides its role as a terminal oxidase, *cbb*$_3$ also functions as a redox sensor to repress the activity of photosynthesis genes under aerobic conditions by controlling the activity of transcriptional regulators of photosynthesis gene expression (29–32). Similarly, the *cbb*$_3$ oxidase of MSR-1 seems to share some functions with the periplasmic nitrate reductase Nap, one of the enzymes involved in poising the redox state for magnetite synthesis (6). This can be concluded from the following observations. (i) A significant growth lag was found for the Δ*cbb*$_3$ and Δ*aa*$_3$ Δ*cbb*$_3$ mutants under aerobic conditions, similar to that for the Δ*nap* mutant (6). The lower growth rates might be due to an excess of the reductant NADH, which needs to be reoxidized by cell maintenance reactions, as also observed for *Rhodobacter capsulatus* and *Paracoccus pantotrophus* cells grown on more reduced carbon sources (35, 36). However, the lower growth rates might also be caused directly by the lower efficiency of *bd* oxidase. (ii) Aberrant cell morphologies of the Δ*cbb*$_3$ and Δ*aa*$_3$ Δ*cbb*$_3$ mutants were found in microaerobic nitrate medium, an observation similar to that for WT cells grown in the more reduced carbon source acetate (6). Thus, we assumed that a more reduced state of intracellular redox occurs in the Δ*cbb*$_3$ and Δ*aa*$_3$ Δ*cbb*$_3$ mutants, and *cbb*$_3$ oxidase is required for dissipating excess

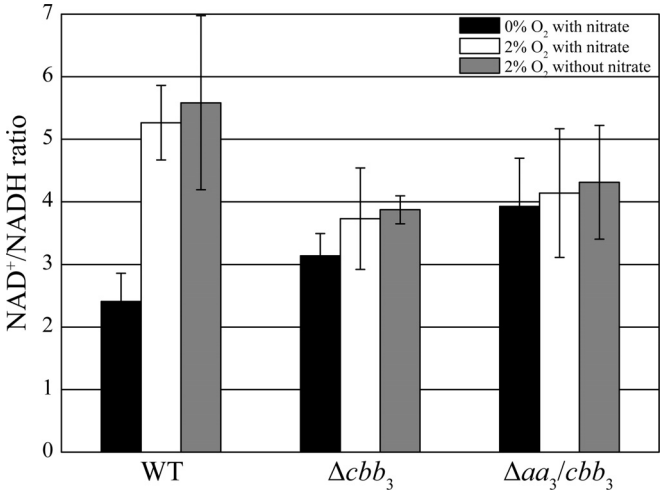

FIG 7 Cellular NAD^+/NADH ratio measurements of WT, Δ*cbb*$_3$, and Δ*aa*$_3$ Δ*cbb*$_3$ strains under different conditions. NAD^+ and NADH were extracted from cells grown in liquid medium, measured, normalized by the luminescence signal, and plotted. Means ± standard deviations are shown ($n = 3$).

reductant. In line with this, in the Δ*cbb*$_3$ and Δ*aa*$_3$ Δ*cbb*$_3$ mutants, the NAD$^+$/NADH ratio under microaerobic conditions was more reduced than that in the WT. Taken together, observations of *cbb*$_3$-deficient cells, including delayed aerobic growth, aberrant cell morphologies, and a reduced redox state under microaerobic conditions, suggest that *cbb*$_3$ oxidase *per se* is able to regulate intracellular redox conditions. This is not surprising, since, as a terminal oxidase, *cbb*$_3$ is capable of accepting electrons during O_2 reduction. However, an optimal redox state (i.e., balanced ratio of Fe^{2+}/Fe^{3+}) seems to be very important for microaerobic biomineralization of the mixed-valence iron oxide magnetite [$Fe(II)Fe(III)_2O_4$], especially in the presence of nitrate, and some other factors involved in magnetite biosynthesis are also likely affected by the loss of *cbb*$_3$ oxidase. For example, several proteins encoded within the genomic magnetosome island, such as MamX, MamZ, and the FtsZ-like protein FtsZm, displayed different defects in magnetosome formation depending on the presence and absence of nitrate (37, 38). MTB contain a unique set of redox-active magnetosome-associated proteins, including MamP, MamX, MamE, and MamT, which share a novel configuration of two close CXXCH heme-binding motifs, the magnetochrome domain (37, 39, 40). Therefore, the change of the intracellular redox state may affect the activity or conformation of these proteins and further impair the redox balance of ferrous and ferric iron for magnetite synthesis. More complex magnetosome phenotypes, such as the presence of two magnetosome chains in the mutants, indicated that vesicle or chain assembly might also be regulated by the cellular redox state. Besides magnetosome-related proteins, the nitrite reductase NirS, which has an Fe(II):nitrite oxidoreductase activity, plays a role in magnetite biomineralization only under low-O_2 conditions and in the presence of nitrate (7). However, more reduced conditions in the Δ*cbb*$_3$ and Δ*aa*$_3$ Δ*cbb*$_3$ mutants likely impair the oxidation of ferrous iron, thereby limiting the concentration of ferric iron for magnetite synthesis and resulting in severely defective magnetosome formation in the presence of nitrate. In addition, variable cell morphologies of microaerobically growing Δ*cbb*$_3$ and Δ*aa*$_3$ Δ*cbb*$_3$ cells in the presence of nitrate, which are likely caused by delayed growth as well as reduced intracellular redox, might be used to adapt to changing conditions.

Although O_2 has been suggested to act as a major factor controlling magnetosome formation for decades, its roles in metabolism and biomineralization in MTB had remained unknown. Our work revealed that in MSR-1, two different branches of the respiration chain occur for O_2 reduction: one is cytochrome *bc*$_1$-*c*-*cbb*$_3$, and the other is the quinol oxidase *bd*, which accepts electrons directly from the quinol pool. Our genetic and biochemical analyses further showed that O_2 respiration is a prerequisite for microaerobic denitrification. Besides its role as a dominant terminal oxidase, *cbb*$_3$ is capable of poising redox conditions, thereby activating denitrification in the presence of oxygen and maintaining a proper redox state for magnetite biomineralization.

ACKNOWLEDGMENTS

We greatly acknowledge the China Scholarship Council (CSC) for financial support of Y.L. and the Brazilian CNPq program for financial support of K.T.S. This work was supported by DFG grant Schu1080/15-1 and HFSP grant RGP0052/2012 to D.S.

REFERENCES

1. **Jogler C, Schüler D.** 2009. Genomics, genetics, and cell biology of magnetosome formation. Annu. Rev. Microbiol. **63:**501–521. http://dx.doi.org/10.1146/annurev.micro.62.081307.162908.
2. **Schübbe S, Kube M, Scheffel A, Wawer C, Heyen U, Meyerdierks A, Madkour MH, Mayer F, Reinhardt R, Schüler D.** 2003. Characterization of a spontaneous nonmagnetic mutant of *Magnetospirillum gryphiswaldense* reveals a large deletion comprising a putative magnetosome island. J. Bacteriol. **185:**5779–5790. http://dx.doi.org/10.1128/JB.185.19.5779-5790.2003.
3. **Ullrich S, Kube M, Schübbe S, Reinhardt R, Schüler D.** 2005. A hypervariable 130-kilobase genomic region of *Magnetospirillum gryphiswaldense* comprises a magnetosome island which undergoes frequent rearrangements during stationary growth. J. Bacteriol. **187:**7176–7184. http://dx.doi.org/10.1128/JB.187.21.7176-7184.2005.
4. **Murat D, Quinlan A, Vali H, Komeili A.** 2010. Comprehensive genetic dissection of the magnetosome gene island reveals the step-wise assembly of a prokaryotic organelle. Proc. Natl. Acad. Sci. U. S. A. **107:**5593–5598. http://dx.doi.org/10.1073/pnas.0914439107.
5. **Lohsse A, Ullrich S, Katzmann E, Borg S, Wanner G, Richter M, Voigt B, Schweder T, Schüler D.** 2011. Functional analysis of the magnetosome island in *Magnetospirillum gryphiswaldense*: the *mamAB* operon is sufficient for magnetite biomineralization. PLoS One **6:**e25561. http://dx.doi.org/10.1371/journal.pone.0025561.
6. **Li Y, Katzmann E, Borg S, Schüler D.** 2012. The periplasmic nitrate reductase Nap is required for anaerobic growth and involved in redox control of magnetite biomineralization in *Magnetospirillum gryphiswaldense*. J. Bacteriol. **194:**4847–4856. http://dx.doi.org/10.1128/JB.00903-12.
7. **Li Y, Bali S, Borg S, Katzmann E, Ferguson SJ, Schüler D.** 2013. Cytochrome *cd*$_1$ nitrite reductase NirS is involved in anaerobic magnetite biomineralization in *Magnetospirillum gryphiswaldense* and requires NirN for proper d_1 heme assembly. J. Bacteriol. **195:**4297–4309. http://dx.doi.org/10.1128/JB.00686-13.
8. **Faivre D, Schüler D.** 2008. Magnetotactic bacteria and magnetosomes. Chem. Rev. **108:**4875–4898. http://dx.doi.org/10.1021/cr078258w.
9. **Faivre D, Agrinier P, Menguy N, Zuddas P, Pachana K, Gloter A, Laval J, Guyot F.** 2004. Mineralogical and isotopic properties of inorganic nanocrystalline magnetites. Geochim. Cosmochim. Acta **68:**4395–4403. http://dx.doi.org/10.1016/j.gca.2004.03.016.
10. **Faivre D, Böttger LH, Matzanke BF, Schüler D.** 2007. Intracellular magnetite biomineralization in bacteria proceeds by a distinct pathway involving membrane-bound ferritin and an iron(II) species. Angew. Chem. Int. Ed. Engl. **46:**8495–8499. http://dx.doi.org/10.1002/anie.200700927.
11. **Abe M.** 2000. Ferrite plating: a chemical method preparing oxide magnetic films at 24-100°C, and its applications. Electrochim. Acta **45:**3337–3343. http://dx.doi.org/10.1016/S0013-4686(00)00403-5.
12. **Zumft WG.** 1997. Cell biology and molecular basis of denitrification. Microbiol. Mol. Biol. Rev. **61:**533–616.
13. **Mandernack KW, Bazylinski D, Shanks WC, Bullen TD.** 1999. Oxygen and iron isotope studies of magnetite produced by magnetotactic bacteria. Science **285:**1892–1896. http://dx.doi.org/10.1126/science.285.5435.1892.
14. **Heyen U, Schüler D.** 2003. Growth and magnetosome formation by microaerophilic *Magnetospirillum* strains in an oxygen-controlled fermentor. Appl. Microbiol. Biotechnol. **61:**536–544. http://dx.doi.org/10.1007/s00253-002-1219-x.
15. **O'Brien W, Paoletti L, Blakemore R.** 1987. Spectral analysis of cytochromes in *Aquaspirillum magnetotacticum*. Curr. Microbiol. **15:**121–127. http://dx.doi.org/10.1007/BF01577258.
16. **Tamegai H, Yamanaka T, Fukumori Y.** 1993. Purification and properties of a 'cytochrom a_1'-like hemoprotein from a magnetotactic bacterium, *Aquaspirillum magnetotacticum*. Biochim. Biophys. Acta **1158:**237–243.
17. **Tamegai H, Fukumori Y.** 1994. Purification and some molecular and enzymatic features of a novel *ccb*-type cytochrome *c* oxidase from a microaerobic denitrifier, *Magnetospirillum magnetotacticum*. FEBS Lett. **347:**22–26. http://dx.doi.org/10.1016/0014-5793(94)00500-1.
18. **Thöny-Meyer L.** 1997. Biogenesis of respiratory cytochromes in bacteria. Microbiol. Mol. Biol. Rev. **61:**337–376.
19. **Saraste M.** 1990. Structural features of cytochrome oxidase. Q. Rev. Biophys. **23:**331–366. http://dx.doi.org/10.1017/S0033583500005588.
20. **Garcia-Horsman JA, Barquera B, Rumbley J, Ma J, Gennis RB.** 1994. The superfamily of heme-copper respiratory oxidases. J. Bacteriol. **176:**5587–5600.

21. **Pitcher RS, Watmough NJ.** 2004. The bacterial cytochrome *cbb*$_3$ oxidases. Biochim. Biophys. Acta **1655:**388–399. http://dx.doi.org/10.1016/j.bbabio.2003.09.017.
22. **VanOrsdel CE, Bhatt S, Allen RJ, Brenner EP, Hobson JJ, Jamil A, Haynes BM, Genson AM, Hemm MR.** 2013. The *Escherichia coli* CydX protein is a member of the CydAB cytochrome *bd* oxidase complex and is required for cytochrome *bd* oxidase activity. J. Bacteriol. **195:**3640–3650. http://dx.doi.org/10.1128/JB.00324-13.
23. **Poole RK, Cook GM.** 2000. Redundancy of aerobic respiratory chains in bacteria? Routes, reasons and regulation. Adv. Microb. Physiol. **43:**165–224. http://dx.doi.org/10.1016/S0065-2911(00)43005-5.
24. **Schüler D, Baeuerlein E.** 1998. Dynamics of iron uptake and Fe_3O_4 biomineralization during aerobic and microaerobic growth of *Magnetospirillum gryphiswaldense*. J. Bacteriol. **180:**159–162.
25. **Sambrook J, Russel DW.** 2001. Molecular cloning: a laboratory manual, 3rd ed. Cold Spring Harbor Laboratory Press, Cold Spring Harbor, NY.
26. **Marrs B, Gest H.** 1973. Genetic mutations affecting the respiratory electron-transport system of the photosynthetic bacterium *Rhodopseudomonas capsulata*. J. Bacteriol. **114:**1045–1051.
27. **Bueno E, Mesa S, Bedmar EJ, Richardson DJ, Delgado MJ.** 2012. Bacterial adaptation of respiration from oxic to microoxic and anoxic conditions: redox control. Antioxid. Redox Signal. **16:**819–852. http://dx.doi.org/10.1089/ars.2011.4051.
28. **Sakaguchi T, Arakaki A, Matsunaga T.** 2002. *Desulfovibrio magneticus* sp. nov., a novel sulfate-reducing bacterium that produces intracellular single-domain-sized magnetite particles. Int. J. Syst. Evol. Microbiol. **52:**215–221. http://ijs.sgmjournals.org/content/52/1/215.long.
29. **Oh JI, Kaplan S.** 2001. Generalized approach to the regulation and integration of gene expression. Mol. Microbiol. **39:**1116–1123. http://dx.doi.org/10.1111/j.1365-2958.2001.02299.x.
30. **O'Gara JP, Kaplan S.** 1997. Evidence for the role of redox carriers in photosynthesis gene expression and carotenoid biosynthesis in *Rhodobacter sphaeroides* 2.4.1. J. Bacteriol. **179:**1951–1961.
31. **O'Gara JP, Eraso JM, Kaplan S.** 1998. A redox-responsive pathway for aerobic regulation of photosynthesis gene expression in *Rhodobacter sphaeroides* 2.4.1. J. Bacteriol. **180:**4044–4050.
32. **Oh JI, Kaplan S.** 2002. Oxygen adaptation. The role of the CcoQ subunit of the *cbb*$_3$ cytochrome *c* oxidase of *Rhodobacter sphaeroides* 2.4.1. J. Biol. Chem. **277:**16220–16228. http://dx.doi.org/10.1074/jbc.M200198200.
33. **Zhou G, Yin J, Chen H, Hua Y, Sun L, Gao H.** 2013. Combined effect of loss of the *caa*$_3$ oxidase and Crp regulation drives *Shewanella* to thrive in redox-stratified environments. ISME J. **7:**1752–1763. http://dx.doi.org/10.1038/ismej.2013.62.
34. **Flies CB, Jonkers HM, de Beer D, Bosselmann K, Böttcher ME, Schüler D.** 2005. Diversity and vertical distribution of magnetotactic bacteria along chemical gradients in freshwater microcosms. FEMS Microbiol. Ecol. **52:**185–195. http://dx.doi.org/10.1016/j.femsec.2004.11.006.
35. **Richardson DJ, King GF, Kelly DJ, McEwan AG, Ferguson SJ, Jackson JB.** 1988. The role of auxiliary oxidants in maintaining redox balance during phototrophic growth of *Rhodobacter capsulatus* on propionate or butyrate. Arch. Microbiol. **150:**131–137. http://dx.doi.org/10.1007/BF00425152.
36. **Ellington MJ, Bhakoo KK, Sawers G, Richardson DJ, Ferguson SJ.** 2002. Hierarchy of carbon source selection in *Paracoccus pantotrophus*: strict correlation between reduction state of the carbon substrate and aerobic expression of the *nap* operon. J. Bacteriol. **184:**4767–4774. http://dx.doi.org/10.1128/JB.184.17.4767-4774.2002.
37. **Raschdorf O, Müller FD, Posfai M, Plitzko JM, Schüler D.** 2013. The magnetosome proteins MamX, MamZ and MamH are involved in redox control of magnetite biomineralization in *Magnetospirillum gryphiswaldense*. Mol. Microbiol. **89:**872–886. http://dx.doi.org/10.1111/mmi.12317.
38. **Müller FD, Raschdorf O, Nudelman H, Messerer M, Katzmann E, Plitzko JM, Zarivach R, Schüler D.** 2014. The FtsZ-like protein FtsZm of *Magnetospirillum gryphiswaldense* likely interacts with its generic homolog and is required for biomineralization under nitrate deprivation. J. Bacteriol. **196:**650–659. http://dx.doi.org/10.1128/JB.00804-13.
39. **Siponen MI, Adryanczyk G, Ginet N, Arnoux P, Pignol D.** 2012. Magnetochrome: a *c*-type cytochrome domain specific to magnetotatic bacteria. Biochem. Soc. Trans. **40:**1319–1323. http://dx.doi.org/10.1042/BST20120104.
40. **Siponen MI, Legrand P, Widdrat M, Jones SR, Zhang WJ, Chang MCY, Faivre D, Arnoux P, Pignol D.** 2013. Structural insight into magnetochrome-mediated magnetite biomineralization. Nature **502:**681–684. http://dx.doi.org/10.1038/nature12573.
41. **Raschdorf O, Plitzko JM, Schüler D, Müller FD.** 9 May 2014. A tailored *galK* counterselection system for efficient markerless gene deletion and chromosomal tagging in *Magnetospirillum gryphiswaldense*. Appl. Environ. Microbiol. http://dx.doi.org/10.1128/AEM.00588-14.